Assessing the Performance of Dynamic World Features in Regional Mangrove Mapping Leveraging Google Earth Engine

S.T. Nyein [1*], A.S. Chia [1], and S.C. Liew[1]

[1] Centre for Remote Imaging Sensing and Processing (CRISP), National University of Singapore 10 Lower Kent Ridge Road, Blk S17 Level 2, Singapore 119076

nyein.st@nus.edu.sg

***Abstract*:** *Mangrove forests in the per-humid insular Southeast Asia region have undergone significant changes resulting from anthropogenic and natural disturbances over the past four decades. Accurate and near real-time mapping of mangrove extent at the regional level plays an important role in conservation efforts. This study assesses the use of Google's Dynamic World (DW) derivatives in regional mangrove mapping using Google Earth Engine (GEE). Dynamic World provides near real-time land cover data with probability layers for various land cover types. We developed three Random Forest (RF) models for mangrove mapping: (1) a model trained using 25960 points with Sentinel-2 imagery, (2) a model trained by combining Sentinel-2 bands with DW probability layers using the same 25960 points, and (3) a model trained over Sentinel-2 bands and DW probability layers with only a few hundred points for monthly or seasonal mapping. The first model achieved an overall accuracy of 96.73%, while the second one achieved 97.72%. Our results show that high-quality and extensive training data are imperative to the performance of RF-based mangrove models, and the addition of DW probability layers slightly improved the model accuracy. However, the model trained solely using DW features would still have limitations at the regional level.*

Keywords: Mangrove, Sentinel-2, Dynamic World, Machine Learning, Google Earth Engine

Introduction

Mangrove forests are one of the most biologically diverse and productive ecosystems on earth which not only provide costal protection and plays a pivotal role in combating global warming due to their efficient carbon sequestration and storage (Field et al., 1998; Alongi et al., 2012). These forests can store five times more carbon in the below-ground compared to other tropical forest ecosystems (Donato et al., 2011). Southeast Asia, which includes both mainland and insular regions fosters the highest mangrove species diversity and encompasses over one-third of the world's mangrove forests (Spalding, 2010; Giri et al., 2010).

Despite their value and importance, mangrove forests in the per-humid insular Southeast Asia region have undergone significant changes resulting from anthropogenic and natural disturbances over the past four decades. Deforestation in insular Southeast Asia has continued at a high rate since the year 2000 because of the significant land use land cover (LULC) changes (Miettinen et al., 2011). Mangrove forests in Southeast Asia are highly susceptible to deforestation and the primary drivers are aquaculture, rice cultivation, and expansion of oil palm and other plantations. Significant mangrove deforestation occurred in Indonesia and Malaysia due to their extensive expansion of oil palm plantations, to keep their status as the top producers of the palm oil. These are further encouraged by the governments for economic development (Richards et al., 2016). Thus, sustainable land use planning and policy implementation are crucial to conserve the mangrove forests in the region and the near real-time mangrove maps play a vital role in addressing the current problem at hand.

Traditional land cover and mangrove mapping methods have extensively relied on various satellite data and human expertise. In recent years, cloud-based platforms like Google Earth Engine (GEE) have revolutionized earth observation by providing powerful tools for large-scale environmental monitoring (Gorelick et al., 2017). As a result of advancement in open datasets and cloud computing, many research groups published the global LULC datasets. Nonetheless, a study (Venter et al., 2022) has shown that the worldwide significant discrepancies lie in these three published LULC datasets in 2020 including ESA World Cover (Zanaga et al., 2021), ESRI's Land Cover (Karra et al., 2021), and Google Dynamic World (DW) (Brown et al., 2022).

Among the recent global LULC datasets, DW provides near real-time 10-m resolution land cover based on Sentinal-2 Top-of-Atmosphere imagery generated using globally trained deep learning model. DW has 8 land cover classes and produce per-class probability layers for various land cover types which can integrate to the different scale mapping (Brown et al., 2022). Near real-time data from DW has the potential to improve the accuracy of land cover classes across the regions and uncertainty estimation (Singh et al., 2024; Ahmed et al., 2024). Moreover, its effectiveness in mangrove mapping in Southeast Asia region has not been thoroughly evaluated.

In this study, we aim to assess the performance of Dynamic World probability layers in regional mangrove mapping using GEE. We developed three Random Forest (RF) models for mangrove mapping: (1) a model trained using 25960 points with Sentinel-2 imagery, (2) a model trained by combining Sentinel-2 bands with DW probability layers using the

same 25960 points, and (3) a model trained over Sentinel-2 bands and DW probability layers with only a few hundred points for monthly or seasonal mapping. After that, we compared three Random Forest (RF) models to evaluate the limitation and advancement of DW integrated regional mangrove mapping models.

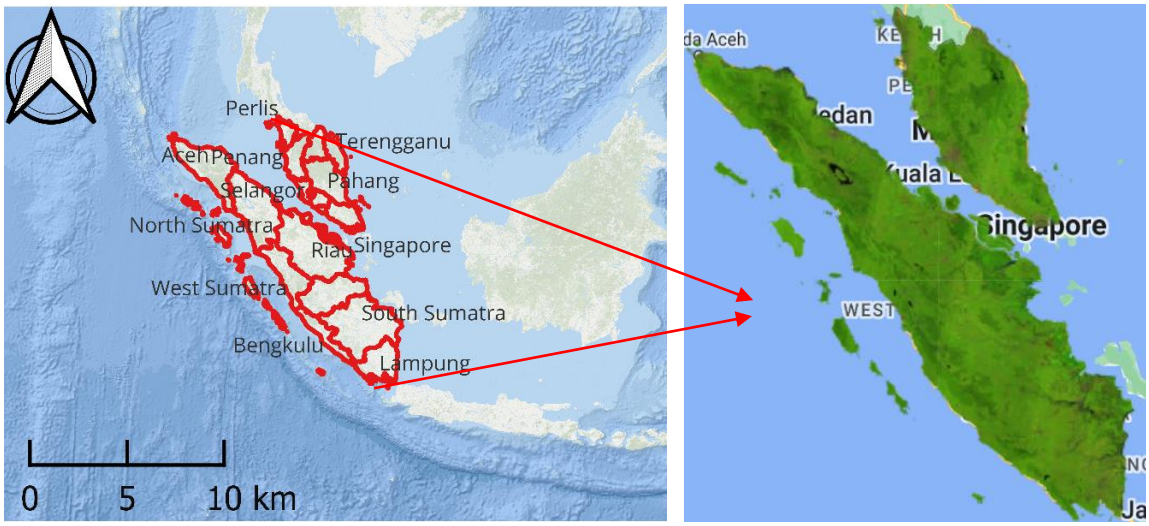

Figure 1: Location of the study area and 2020 Annual False Color Composite of 10 m Sentinel-2 image (Shortwave Infrared, Near Infrared, and Red bands).

Study Area

The study area includes Peninsular Malaysia, Singapore and Indonesia's Sumatra which are parts of the insular Southeast Aisa. The mangrove area in the region encompasses extensive coastlines and is home to significant biodiversity. Western coastal areas of Peninsula Malaysia like Matang Mangrove Forest Reserve, covers over more than 40,000ha and have a vast number of species (Ibharim et al., 2015). Sumatra is the second largest Indonesia island covered by mangrove areas and have one of the most biodiverse and expansive mangrove forests in Southeast Asia, especially along the eastern coastline (Basyuni et al., 2022). The reason for selecting this region as a study area is because it stands for a significant amount of mangrove forest in insular Southeast Asia region that faces mangrove deforestation and degradation due to the rapid changes in land use land cover.

Methodology

We used Sentinel-2 Level-2A orthorectified atmospherically corrected surface reflectance imagery for our mangrove mapping models. First, we created an annual cloud-free

Sentinel-2 composite for the year 2020 with red, green, blue, near infrared (nir), shortwave infrared 1 (swir1), shortwave infrared 2 (swir2), red edge 1 (re1), red edge 2 (re2), and red edge 3 (re3) bands to train our mangrove models. The reference points are collected by visual interpretation using Sentinel-2 and Planet images of 2020 with the 2015 mangrove layer from our existing land cover map. There are a total of 25960 reference points including 12258 mangrove and 13702 non-mangrove labels (Fig. 2).

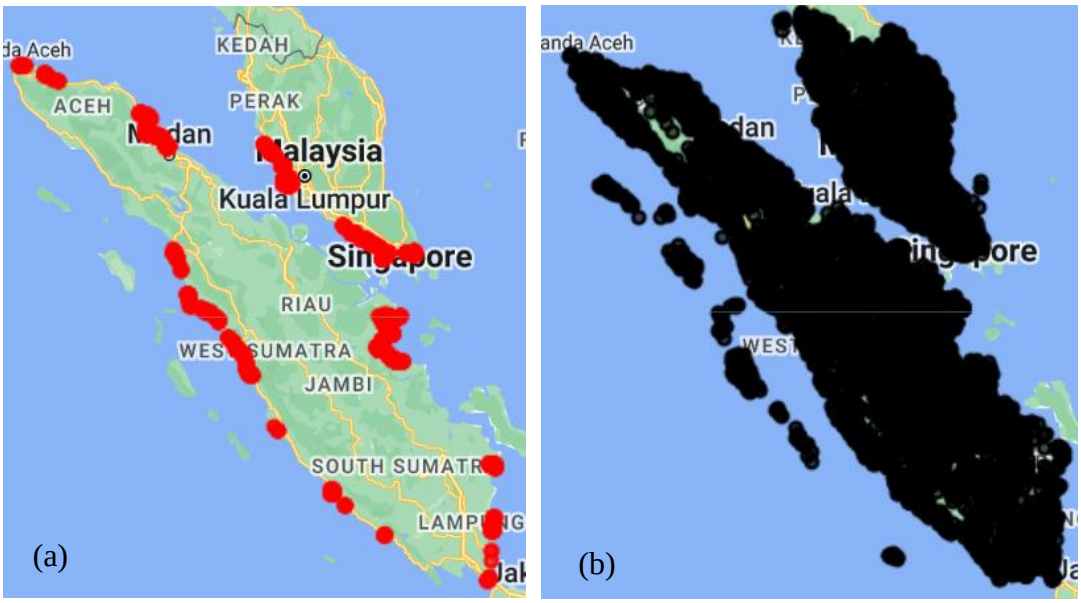

Figure 2: Reference points of (a) mangrove and (b) non-mangrove

We developed three Random Forest (RF) models for mangrove mapping: (1) a model trained using 25960 points with Sentinel-2 imagery, (2) a model trained by combining Sentinel-2 bands with DW probability layers using the same 25960 points, and (3) a model trained over Sentinel-2 bands and DW probability layers with only a few hundred points. The objective of the first two models is to study whether adding DW probability layers as the extra features might be able improve our existing regional model with extensive reference dataset or not. The motivation of the third model is to evaluate how DW probability layers are feasible and dependable for near real-time or seasonal mangrove mapping purposes with only a few collected points.

In addition, different normalized difference (ND) of Sentinel-2 6 bands were calculated and there are more common names for some bands combination such as and Normalized Difference Vegetation Index (NDVI, Rouse et al., 1974) Normalized Difference Water Index (NDWI, McFeeters, 1996), Normalized Burn Ratio (NBR, Key and Benson, 1999), and Normalized Difference Snow Index (NDSI, Salomonson and Appel, 2004). Further, we also included the Enhanced Vegetation Index (EVI, Jiang et al., 2008) and the Soil-

adjusted vegetation index (SAVI, Huete, 1988) and Index-based Built-Up Index (IBI, Xu, 2008), the terrain indices derived from SRTM (Farr et al., 2007), the Tasseled Cap transformation derivatives (Crist and Cicone, 1984), and other ancillary data like distance to coast calculated from Open Street Map (OSM, 2017). Detailed information of features used to train the models is described detailed in Table 2.

The reference dataset is divided into 70% for training and 30% for testing of the model. Model 1 was trained using 45 features and model 2 employed 54 features. After the initial training of each model, the feature importance of the Random Forest model was assessed, and the top 20 most important features were selected for the final model training. Model 3 utilized only 18 features derived from Sentinel-2 bands and DW probability layers and trained using 188 points of mangrove and 234 points of non-mangrove labels. For the accuracy assessment, we performed model validation using 30% of the reference data and visual comparison with Global Mangrove Watch (GMW, Bunting et al., 2022) data in 2020.

Results

The proposed 3 mangrove models were implemented leveraging built-in RF algorithm in GEE. Model 1 achieved the overall accuracy of 96.73% while model 2 slightly improved the overall accuracy by 97.72%. Model 3 resulted the overall accuracy of 79.49% with 87.25% precision and 71.77% recall. The detailed metrics are shown in Table 1 and the accuracy assessment was done only with 30% of testing data. Therefore, the models' accuracy might be influenced by the bias from the dataset and spatial distribution of the reference data.

Table 1: Accuracy assessment of 3 mangrove models

Model	Precision (%)	Recall (%)	Overall Accuracy (%)
Model 1	96.80	96.29	96.73
Model 2	97.80	97.37	97.72
Model 3	87.25	71.77	79.49

Figure 3 presents the results of three different mangrove models with sentinel-2 false color composite and column (b), (c), and (d) describes the probability layers of the models. White color in the results represents the lowest probability 0-10% and purple color represents the highest probability 90-100%. We also compared our results with the 2020 GMW's mangrove extent layer. The first three rows display the outputs for Matang, Klang islands, and Sungai

Pulai mangrove forest reserves in Malaysia and all models effectively detect the mangrove forest areas within these regions when we compared with GMW layer. The last three rows reveal the results of mangrove forests detected in North Sumatra, Riau, and South Sumatra in Indonesia. The models performed well in most mangrove areas, though Model 3 showed some misclassification, identifying plantation areas as mangrove in certain areas.

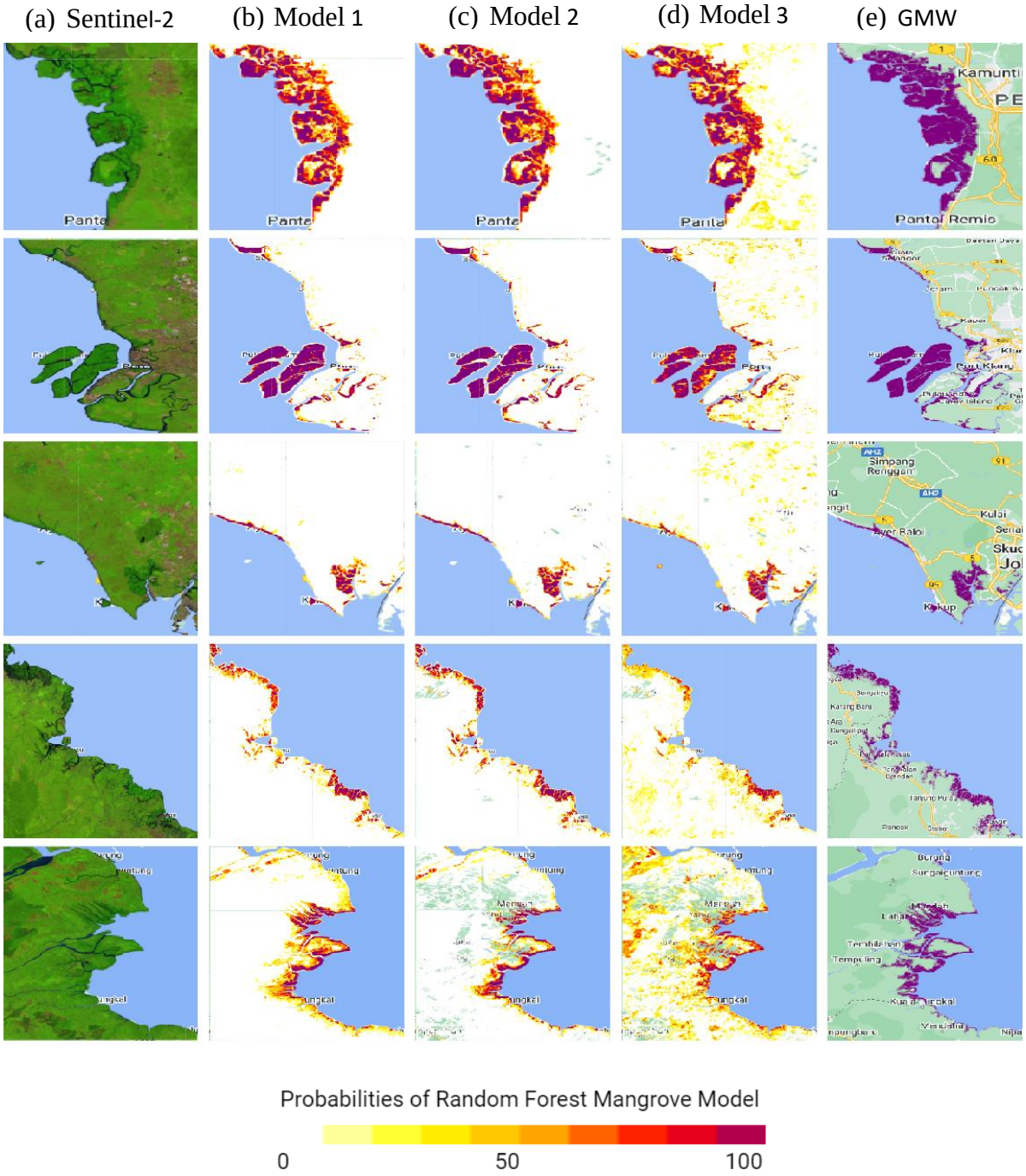

Figure 3: Results of the different mangrove models in 2020 and comparison with GMW 2020 data. (a) Sentinel-2 False Color Composite, (b) Probability layer of Model 1, (c) Probability layer of Model 2, (d) Probability layer of Model 3, and (e) 2020 GMW layer

Conclusion

In conclusion, this study shows that Google's DW features may improve regional mangrove mapping. Though integrating DW probability layers as extra features in our model slightly improved the accuracy, the increase from 96.73% to 97.72% between Model 1 and Model 2 may not be statistically significant. While DW's probability derivatives slightly enhance the model performance, they are not sufficient to train their own model for the near real-time purpose and cloud coverage remains an issue for the tropical region. Further modification of the model and independent validation for accuracy assessment would be necessary to fully harness DW features to develop reliable mangrove mapping model.

Table 2: List of features used to train the three mangrove models

Model 1	Model 2	Model 3
red	red	red
green	green	green
blue	blue	blue
nir	nir	nir
swir1	swir1	swir1
swir2	swir2	swir2
re1	re1	re1
re2	re2	re2
re3	re3	re3
ND_blue_green	ND_blue_green	bare
ND_blue_red	ND_blue_red	built
ND_blue_nir	ND_blue_nir	crops
ND_blue_swir1	ND_blue_swir1	grass
ND_blue_swir2	ND_blue_swir2	flooded_vegetation
ND_green_red	ND_green_red	shrub_and_scrub
ND_green_nir	ND_green_nir	snow_and_ice
ND_green_swir1	ND_green_swir1	trees
ND_green_swir2	ND_green_swir2	water
ND_red_swir1	ND_red_swir1	
ND_red_swir2	ND_red_swir2	
ND_nir_red	ND_nir_red	
ND_nir_swir1	ND_nir_swir1	
ND_nir_swir2	ND_nir_swir2	
ND_swir1_swir2	ND_swir1_swir2	
EVI	EVI	
SAVI	SAVI	

IBI	IBI	
brightness	brightness	
greenness	greenness	
wetness	wetness	
fourth	fourth	
fifth	fifth	
sixth	sixth	
tcAngleBG	tcAngleBG	
tcAngleGW	tcAngleGW	
tcAngleBW	tcAngleBW	
tcDistanceBG	tcDistanceBG	
tcDistanceGW	tcDistanceGW	
tcDistanceBW	tcDistanceBW	
distCoast	distCoast	
elevation	elevation	
slope	slope	
aspect	aspect	
eastness	eastness	
nortness	nortness	
	bare	
	built	
	crops	
	grass	
	flooded_vegetation	
	shrub_and_scrub	
	snow_and_ice	
	trees	
	water	

References

Ahmed, R., Zafor, M. A., & Trachte, K. (2024). Land-Use and Land-Cover changes in Cottbus City and Spree-Neisse District, Germany, in the last two decades: a study using remote sensing data and Google Earth engine. Remote Sensing, 16(15), 2773.

Alongi, D. M. (2012). Carbon sequestration in mangrove forests. Carbon management, 3(3), 313-322.

Basyuni, M., Sasmito, S. D., Analuddin, K., Ulqodry, T. Z., Saragi-Sasmito, M. F., Eddy, S., & Milantara, N. (2022). Mangrove biodiversity, conservation and roles for livelihoods in Indonesia. In Mangroves: Biodiversity, livelihoods and conservation (pp. 397-445). Singapore: Springer Nature Singapore.

Brown, C. F., Brumby, S. P., Guzder-Williams, B., Birch, T., Hyde, S. B., Mazzariello, J., Czerwinski, W., Pasquarella, V. J., Haertel, R., Ilyushchenko, S., Schwehr, K., Weisse, M.,

Stolle, F., Hanson, C., Guinan, O., Moore, R., & Tait, A. M. (2022). Dynamic World, Near real-time global 10 m land use land cover mapping. Scientific Data, 9(1).

Bunting, Pete, Rosenqvist, Ake, Hilarides, Lammert, Lucas, Richard, Thomas, Nathan, Tadono, Takeo, Worthington, Thomas, Spalding, Mark, Murray, Nicholas, & Rebelo, Lisa-Maria. (2022). Global Mangrove Watch (1996 - 2020) Version 3.0 Dataset (3.0) [Data set]. Zenodo. https://doi.org/10.5281/zenodo.6894273

Crist, E. P., & Cicone, R. C. (1984). A physically-based transformation of Thematic Mapper data---The TM Tasseled Cap. IEEE Transactions on Geoscience and Remote sensing, (3), 256-263.

Donato, D. C., Kauffman, J. B., Murdiyarso, D., Kurnianto, S., Stidham, M., & Kanninen, M. (2011). Mangroves are among the most carbon-rich forests in the tropics. Nature geoscience, 4(5), 293-297.

Farr, T. G., Rosen, P. A., Caro, E., Crippen, R., Duren, R., Hensley, S., ... & Alsdorf, D. (2007). The shuttle radar topography mission. Reviews of geophysics, 45(2).

Field, C. B., Osborn, J. G., Hoffman, L. L., Polsenberg, J. F., Ackerly, D. D., Berry, J. A., Bjorkman, O., Held, A., Matson, P. A., & Mooney, H. A. (1998). Mangrove biodiversity and ecosystem function. Global Ecology and Biogeography Letters, 7(1), 3. https://doi.org/10.2307/2997693

Giri, C., Ochieng, E., Tieszen, L. L., Zhu, Z., Singh, A., Loveland, T., Masek, J., & Duke, N. (2010). Status and distribution of mangrove forests of the world using earth observation satellite data. Global Ecology and Biogeography, 20(1), 154–159.

Gorelick, N., Hancher, M., Dixon, M., Ilyushchenko, S., Thau, D., & Moore, R. (2017). Google Earth Engine: Planetary-scale geospatial analysis for everyone. Remote sensing of Environment, 202, 18-27.

Huete, A. R. (1988). A soil-adjusted vegetation index (SAVI). Remote sensing of environment, 25(3), 295-309.

Ibharim, N., Mustapha, M., Lihan, T., & Mazlan, A. (2015). Mapping mangrove changes in the Matang Mangrove Forest using multi temporal satellite imageries. Ocean & Coastal Management, 114, 64–76.

Jiang, Z., Huete, A. R., Didan, K., & Miura, T. (2008). Development of a two-band enhanced vegetation index without a blue band. Remote sensing of Environment, 112(10), 3833-3845.

Karra, K., Kontgis, C., Statman-Weil, Z., Mazzariello, J. C., Mathis, M., & Brumby, S. P. (2021). Global land use/land cover with Sentinel 2 and deep learning. In 2021 IEEE international geoscience and remote sensing symposium IGARSS (pp. 4704-4707). IEEE.

Key, C. H., & Benson, N. C. (1999). The Normalized Burn Ratio (NBR): A Landsat TM radiometric measure of burn severity. United States Geological Survey, Northern Rocky Mountain Science Center: Bozeman, MT, USA.

McFeeters, S. K. (1996). The use of the Normalized Difference Water Index (NDWI) in the delineation of open water features. International journal of remote sensing, 17(7), 1425-1432.

Miettinen, J., Shi, C., & Liew, S. C. (2011). Deforestation rates in insular Southeast Asia between 2000 and 2010. Global change biology, 17(7), 2261-2270.

OpenStreetMap Contributors, 2017. Planet Dump. Retrieved from: https://www.planet.osm.org, https://www.openstreetmap.org

Richards, D. R., & Friess, D. A. (2016). Rates and drivers of mangrove deforestation in Southeast Asia, 2000–2012. Proceedings of the National Academy of Sciences, 113(2), 344-349.

Rouse, J. W., Haas, R. H., Schell, J. A., & Deering, D. W. (1974). Monitoring vegetation systems in the Great Plains with ERTS. NASA Spec. Publ, 351(1), 309.

Salomonson, V. V., & Appel, I. (2004). Estimating fractional snow cover from MODIS using the normalized difference snow index. Remote sensing of environment, 89(3), 351-360.

Singh, G., Moncrieff, G., Venter, Z., Cawse-Nicholson, K., Slingsby, J., & Robinson, T. B. (2024). Uncertainty quantification for probabilistic machine learning in earth observation using conformal prediction. Scientific Reports, 14(1).

Spalding, M. (2010). World atlas of mangroves. Routledge.

Venter, Z. S., Barton, D. N., Chakraborty, T., Simensen, T., & Singh, G. (2022). Global 10 m land use land cover datasets: A comparison of dynamic world, world cover and esri land cover. Remote Sensing, 14(16), 4101.

Xu, H. (2008). A new index for delineating built-up land features in satellite imagery. International journal of remote sensing, 29(14), 4269-4276.

Zanaga, D., Van De Kerchove, R., Daems, D., De Keersmaecker, W., Brockmann, C., Kirches, G., Wevers, J., Cartus, O., Santoro, M., Fritz, S., Lesiv, M., Herold, M., Tsendbazar, N., Xu, P., Ramoino, F., & Arino, O. (2022). ESA WorldCover 10 m 2021 v200.